Carbohydrate Polymers 87 (2012) 210–217

Contents lists available at ScienceDirect

Carbohydrate Polymers

journal homepage: www.elsevier.com/locate/carbpol

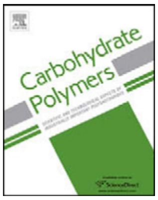

Xylose production from giant reed (*Arundo donax* L.): Modeling and optimization of dilute acid hydrolysis

Anatoly A. Shatalov*, Helena Pereira

Forest Research Center, Institute of Agronomy, Technical University of Lisbon, Tapada da Ajuda, 1349-017 Lisbon, Portugal

ARTICLE INFO

Article history:
Received 28 April 2011
Received in revised form 18 July 2011
Accepted 22 July 2011
Available online 30 July 2011

Keywords:
Heteroxylan
Acid hydrolysis
Statistical modeling
Xylose
Giant reed
Biorefinery

ABSTRACT

Statistical modeling and optimization of dilute sulfuric acid hydrolysis of potential energy crop giant reed (*Arundo donax* L.) has been performed using response surface methodology. Central composite rotatable design was applied to assess the effect of acid concentration, reaction time and temperature on efficiency and selectivity of xylan polysaccharide conversion to xylose. Second-order polynomial model was fitted to experimental data to find the optimum reaction conditions by multiple regression analysis. The monomeric xylose recovery ca. 94% (vs. 93% predicted) was achieved under optimized hydrolysis conditions (1.27% acid concentration, 141.6 °C and 36.4 min), confirming the high validity of the developed model. The low content of glucose (2.7%) and monosaccharide degradation products (0.9% furfural and 0.7% 5-hydroxymethylfurfural) provided a high quality xylose-rich subtract, ready for subsequent biochemical conversion to value-added products. The solid xylan-free residue was easily converted to fermentable sugars resulting in cellulose digestibility of 70% vs. 9% for untreated biomass.

1. Introduction

The critical issues of global energy security and climate change associated with fast depletion of fossil resources and greenhouse gas emissions from fossil fuels combustion stimulated great interest in exploring of alternative (renewable) energy sources, such as biomass. The multi-stage fractionation/conversion of different biomass feedstocks to fuel and other products, i.e., the biorefinery concept of biomass processing, is being considered now as a more potential way to guarantee sustainable bio-based economy (Fernando, Adhikari, Chandrapal, & Murali, 2006; Kamm & Kamm, 2007) Particularly, the lignocellulosic feedstock (LCF) biorefinery, that uses cellulose-containing biomass and wastes, has been the focus of much attention for the last few years, as a more successful large-scale biorefinery scheme (Kamm et al., 2006).

The agro-based lignocellulosics, such as industrial crop residues and various grasses represent an abundant and cheap feedstock for LCF biorefinery (FitzPatrick, Champagne, Cunningham, & Whitney, 2010). Perennial rhizomatous grasses, having high yield potential and low input demands, can be the perfect candidates to fulfil the needs of biofuel and biochemicals production. Among a variety of herbaceous species evaluated as potential energy crops in both the US and Europe, four perennial rhizomatous grasses such as switchgrass (*Panicum virgatum*), miscanthus (*Miscanthus* spp.), reed canary grass (*Phalaris arundinacea*) and giant reed (*Arundo donax*) showed the best potential for biomass production and were chosen for more extensive research programs (Lewandowski, Scurlock, Lindvall, & Christou, 2003).

A. donax L. is a perennial reed species native to southern Europe (Mediterranean region) and widely distributed into all subtropical and warm temperate areas of the world (Perdue, 1958). Being introduced into North America in the late 1800s, it now grows wild and cultivated in California and other southern regions of the US. The high biomass productivity (reported yields up to 63 and 67 t year^{-1} ha^{-1} of dry matter in Europe and US, respectively) (Hidalgo & Fernandez, 2001; Lewis & Jackson, 2002), annual harvesting period, easy adaptability to different soil and climatic conditions, ability to intensive cultivation and appropriate chemical composition make this grass as a very potential energy crop for industrial utilization and particularly attractive lignocellulosic feedstock for LCF biorefinery schemes. The recent utilization of giant reed for delignification (pulp production) (Shatalov & Pereira, 2006), auto-hydrolysis (as a pre-delignification step) (Caparrós, Ariza, Hernanz, & Díaz, 2006; Caparrós, Garrote, Ariza, & López, 2006) and pyrolysis (char production) (Bassoa, Cerrellaa, Buonomoa, Bonellia, & Cukiermana, 2005) has been reported.

Since the carbohydrate fraction accounts for up to 80% of lignocellulosic raw materials (Kamm & Kamm, 2007) the efficient access and conversion of carbohydrates to chemical bulk products (industrial intermediates) and the corresponding final products is a key factor for successful commercialization of LCF biorefinery (Zhang,

---

* Corresponding author. Tel.: +351 21 3653379; fax: +351 21 3653338.
E-mail address: anatoly@isa.utl.pt (A.A. Shatalov).

0144-8617/$ – see front matter © 2011 Elsevier Ltd. All rights reserved.
doi:10.1016/j.carbpol.2011.07.041

2008). Hemicelluloses are the second (after cellulose) most abundant polysaccharides in lignocellulosics (20–35%), and the xylan is the most abundant polysaccharide in hemicelluloses (Saha, 2003). In agro-based biomass the proportion of xylan may amount to 95% of the total non-cellulosic polysaccharides (Hurter, 1988). The monomeric xylose can be used as substrate for production a wide variety of products, such as xylitol, a five-carbon sugar alcohol that has attracted much attention because of its potential use in food and pharmaceutics (as a natural food sweetener, dental caries reducer, sugar substitute for diabetics, thin coating of tablets) (Granström & Leisola, 2009). Xylan isolation and depolymerization to xylose can therefore be an important first step (entry point) in the complex biorefinery scheme. The dilute sulfuric acid hydrolysis under moderate reaction conditions was proved to be a reliable and easily performed low cost method for quantitative conversion of hemicellulosic xylan to monomeric sugars and enzymatic digestibility improvement of residual cellulose. Hemicellulose hydrolysis of different lignocellulosic biomass by dilute sulfuric acid solutions has been reported (Akpinar, Levent, Bostanci, Bakir, & Yilmaz, 2011; Dien et al., 2006; Esteghlalian, Hashimoto, Fenske, & Penner, 1997; Guo, Chen, Chen, Men, & Hwang, 2008; Jeong, Um, Kim, & Oh, 2010; Rahman, Choudhury, Ahmad, & Kamaruddin, 2007). The results showed that the amount of sugars released during hydrolysis is dependent on the type of raw material used and operational conditions (reaction time, temperature and acid concentration) applied for hydrolysis reaction. The minimal monosaccharide decomposition to furans and cellulose degradation can be achieved under optimized conditions, providing high effectiveness and selectivity of the overall hydrolysis process.

The xylose production from potential energy crop giant reed (*A. donax* L.) has been studied using a low temperature dilute sulfuric acid hydrolysis. The response surface methodology (RSM) was employed for process modeling and optimization to maximize effectiveness and selectivity of xylan conversion to monomeric xylose within one-step reaction. The present paper reports the principal results of this study.

2. Materials and methods

2.1. Raw material and chemical

Giant reed (*A. donax* L.) was sampled from the naturally growing native crop population (Lisbon, Portugal) with average stem height of 4 m. The air-dry stems were manually stripped of leaves, milled and screened to particle size of 40–60 mesh and stored in sealed plastic bags at room temperature until using.

Commercial enzyme preparations Celluclast 1.5L (cellulases from *Trichoderma reesei*) and Novozyme-188 (β-glucosidases from *Aspergillus niger*) were purchased by Sigma Co. Enzymatic activity (as FPU/mL and *p*NPGU/mL, respectively) (Berghem & Petterson, 1974; Ghose, 1987) was determined before enzyme application.

All other chemicals used were of analytical grade purity and purchased by Sigma, Aldrich and Fluka Co.

2.2. Dilute acid hydrolysis

Hydrolysis experiments (replicated for each condition set) were carried out in the stainless steel digesters (ca. 100 cm^3 cap.) rotated in an oil bath. For optimization study, the digesters were loaded with 5 g (on oven-dry basis) of reed sawdust and 75 ml of sulfuric acid solution. The process variables were reaction time (20–70 min), reaction temperature (120–150 °C) and acid concentration (0.2–1.8%). The heating-up period for each experiment was 3 min. Solid residue after hydrolysis was separated from solution by vacuum-filtration and kept frozen for subsequent analysis and processing. The collected hydrolysate was examined on degree of monosaccharide recovery and degradation. Xylan conversion after hydrolysis (Y_1) was defined as a ratio of xylose content in hydrolysate to xylose content in cardoon. Hydrolysis selectivity (Y_2) was defined as a ratio of xylose to glucose in hydrolysate.

2.3. Enzymatic hydrolysis

The enzymatic digestibility of insoluble lignocellulosic residue after acidic hydrolysis was checked by NREL standard procedure (Selig, Weiss, & Ji, 2008). Residue (0.15 g) was mixed with commercial preparations of cellulases (60 FPU/g cellulose) and β-glucosidases (64 *p*NPGU/g cellulose) in 50 mM sodium citrate buffer (pH 4.8) and incubated at 50 °C for 24–72 h under 150 rpm rotation. Sodium azide (2% solution) was added as antibiotic to prevent any microbial infection during digesting. The release of soluble sugars (basically glucose) was determined by HPLC and corrected by blank tests on substrate and enzymes. The enzymatic digestibility (saccharification) was defined as a ratio of cellulose digested (g) to cellulose added (g).

2.4. Analytical methods

Extractives were determined gravimetrically after successive Soxhlet extraction by dichloromethane, ethanol and water. Ash, silica (as SiO_2), acid-insoluble (Klason) and acid-soluble lignin were determined according to TAPPI T15 os 58, TAPPI T 245 om-94, TAPPI T 222 om-88 and TAPPI UM 250 standards, respectively. Holocellulose was isolated by modified chlorite method in the presence of sodium acetate buffer (Browning, 1967). Hemicelluloses were successively extracted from holocellulose by 5% and 24% potassium hydroxide solutions and recovered by ethanol addition, giving, respectively, fractions A and B. The insoluble residue after alkaline extraction of holocellulose was defined as α-cellulose (Browning, 1967). Monosaccharide composition of holocellulose and hemicelluloses was determined by GC as alditol-acetate derivatives (Hewlett Packard 5890), under conditions described elsewhere (Shatalov & Pereira, 2007). The total content of reducing sugars and furans formed in preliminary hydrolysis experiments was determined by DNS method and UV-spectroscopy (Shimadzu UV-160A), respectively (Martinez, Rodriguez, York, Preston, & Ingram, 2000; Miller, 1959). The concentration of xylose, glucose, acetic acid, furfural and 5-hydroxymethylfurfural (HMF) in hydrolysates was quantified by HPLC using Aminex HPX-87H column (Bio-Rad, Hercules, CA, USA) operating at 50 °C, in combination with a cation H^+-guard column (Bio-Rad, Hercules, CA, USA). The mobile phase was 5 mM sulfuric acid and the flow rate 0.4 ml min^{-1}.

2.5. Statistical modeling

Response surface methodology (RSM) was employed for statistical data treatment and optimization of hydrolysis conditions by multiple regression analysis, using Statistica 6.0 (Statsoft, USA) software. The 2^3 central composite rotatable design (CCRD) with three independent variables at five different levels, six star (axial) points and five central points (total 19 runs) was adopted to find linear, quadratic and interaction effects of independent process variables on experimental responses. A second-order polynomial model was fitted to each set of experimental data to predict optimal reaction conditions by following equation:

$$Y = b_0 + \sum_{i=1}^{3} b_i X_i + \sum_{i=1}^{3} b_{ii} X_i^2 + \sum_{i<j,\ j=2}^{3} b_{ij} X_i X_j \qquad (1)$$

where Y is a predicted response (xylan conversion or hydrolysis selectivity), b_0 is an interception coefficient (regression coefficient

Table 1
Chemical composition of giant reed stem-wall material.

Component	Content (% on oven-dry matter)
Ash	5.04 ± 0.03
Silica SiO_2	2.24 ± 0.01
Extractives	12.22 ± 0.19
Dichloromethane	0.36 ± 0.01
Ethanol	4.99 ± 0.28
Water	6.88 ± 0.27
Lignin	24.02 ± 0.04
Acid-insoluble (Klason)	21.85 ± 0.04
Acid-soluble	2.17 ± 0.03
Holocellulose	59.46 ± 0.05
α-Cellulose	33.85 ± 0.06
Hemicelluloses	25.61 ± 0.07
Fraction A	20.99 ± 0.04
Fraction B	4.62 ± 0.05

at central point), b_i are the linear coefficients; b_{ii} are the quadratic coefficients, b_{ij} are the interaction coefficients, X_i and X_j are the independent variables (temperature, time and acid concentration).

The statistical significance of regression coefficients and effects was checked by analysis of variance (ANOVA).

3. Results and discussion

3.1. Compositional analysis of raw material

Detailed chemical analysis of the stem-wall material of giant reed used in this study revealed some general features typical for other industrially important agro-crops and deviations from woody species (Table 1). The content of cellulose, as the principal chemical constituent accounting for about 34% of giant reed stem, does not differ greatly from wheat straw (29–35%), bamboo (26–43%) and sugarcane bagasse (32–44%), but somewhat lower in comparison with woods (38–50%) (Hurter, 1988). Similar to other grasses, giant reed has less lignin (ca. 24%) and more extractives (ca. 12%), as compared with woods (25–30% and 1–5%, respectively) (Atchison, 1987). The particularly high proportion of water-soluble substances (ca. 7%), composed mainly of low-molecular phenolics and pectins (Browning, 1967), indicates the high accessibility and therefore reactivity of giant reed during chemical processing, e.g., in delignification, suggesting application of more gentle reaction conditions and reduced chemical charge. The minerals (ash) comprise ca. 5% (w/w) of the reed stem material, similar to wheat straw (4–9%), flax (2–5%), kenaf (2–5%) and substantially higher of wood species (ca. 1%) (Hurter, 1988). The elevated proportion of alkaline constituents (basic cations) in total ash reported to be common for grasses can partially neutralize the sulfuric acid and lower the acidity of the reaction mixture in acid hydrolysis treatment. The buffering (neutralizing) capacity of the giant reed stem-wall material should be determined first, if the reduced liquid-to-solid ratios (less than 10) are used for acid hydrolysis (Esteghlalian et al., 1997). The content of Si in raw material is of special importance, because of its harmful effect on chemicals and energy recovery from the liquid technological streams. Silicates (as SiO_2) comprise ca. 2.2% of the stem-wall material of giant reed (ca. 44% of total minerals); what is close to common reed *Phragmites communis* Trin. (2%), bamboo (1.5–3%) and bagasse (0.7–3%), but substantially lower of cereals straw, such as wheat (3–7%) or rice (9–14%) (Hurter, 1988).

Structural polysaccharides (holocellulose) account for ca. 60% (w/w) of dry stem matter of giant reed, of which ca. 26% (or 43% of total carbohydrates) falls on hemicelluloses (Table 1). Similar to other industrial agro-crops, the principal non-cellulosic polysaccharide of *A. donax* is heteroxylan (arabino-4-*O*-methylglucuronoxylan) with homopolymeric backbone of 1,4-linked β-D-xylopyranose units and monomeric side-chains of arabinose and glucuronic acid linked to *O*-2 and/or *O*-3 of xylose residues (Joseleau & Barnoud, 1975). As can be seen from Table 2, the proportion of xylan in giant reed stems used in the study reaches up to 89% of total hemicelluloses, what amounts 20.4% of the stem-wall material and gives the value of maximum (theoretical) xylose yield of 23.1% after hydrolysis reaction.

Table 2
Carbohydrate composition of holocellulose and hemicelluloses fraction of giant reed stem-wall material (% of total).

	Holocellulose	Hemicelluloses	
		Fraction A	Fraction B
Rhamnose	0.27	0.60	0.45
Arabinose	2.87	7.62	5.46
Xylose	34.74	88.50	87.22
Mannose	0.58	0.30	0.65
Galactose	0.97	1.21	0.87
Glucose	60.58	1.76	5.34

The obtained data on chemical composition of giant reed stems are in good agreement with previously reported studies, where similar proportion between main chemical constituents (cellulose, hemicelluloses, lignin and extractives) was found (Perdue, 1958; Shatalov, Quilhó, & Pereira, 2001; Verteris, Georghiou, Christodoulakis, Santas, & Santas, 2004).

3.2. Effect of hydrolysis conditions on xylose formation and degradation

A series of preliminary hydrolysis experiments have been carried out under variable conditions of sulfuric acid concentration (0.5, 1.0 and 1.5%), reaction temperature (130, 140 and 150 °C) and reaction time (30 and 60 min) to define the current levels (settings) of the independent process variables to be used in statistical experimental design for process modeling and optimization.

As can be seen from Table 3, although the significant amount of monomeric xylose can be recovered in solution after dilute-acid hydrolysis, the xylose recovery (yield) is highly dependent of applied reaction conditions. In general, increase in process severity (i.e., increase in acid concentration, temperature and duration), while accelerating xylan hydrolysis to xylose, intensifies substantially the secondary degradation reactions of monomeric sugars thereby decreasing the final xylose yield in solution. Some other sugars, such as arabinose and glucose, particularly, are formed during dilute hydrolysis. Whereas arabinose forms a part of heteroxylan structure, the presence of glucose is a result of cellulose degradation, namely, of its less ordered (amorphous) portion having the same (or close) reactivity with hemicelluloses (Fengel & Wegener, 1989). Like the furans, glucose can have harmful effect on subsequent xylose bioconversion, e.g., to xylitol. Hydrolysis selectivity should therefore assure the minimal concentration of glucose units in hydrolyzate as xylose-rich substrate. Obviously, the temperature of 130 °C provides more preserving conditions for the formed monosaccharides and only traces of furfural can be detected in reaction solution (Table 3). Limited cellulose degradation and acetic acid formation (due to splitting out of acid-liable acetic groups of heteroxylan) was also observed. At the same time, the xylose recovery in solution (as a main objective) was low under this process temperature, pointing to incomplete xylan conversion. By contrast, the drastic conditions of 150 °C caused substantial monosaccharide (basically xylose) degradation and cellulose depolymerization (up to 5.3% of furfural and 4% of glucose in solution), decreasing substantially xylose recovery after hydrolysis and lowering substrate quality as a whole, particularly under elevated acid concentration.

Table 3
Experimental data on formation and decomposition of monomeric sugars during hydrolysis of giant reed stalks.

T (°C)	t (min)	C (%)	Yield (% on oven-dry material)					
			Glc[a]	Xyl	Ara	AcA	F	HMF
130	30	0.5	1.91 ± 0.08	7.01 ± 0.13	1.32 ± 0.14	Traces	Traces	Traces
		1.0	2.18 ± 0.15	15.28 ± 0.18	1.53 ± 0.13	1.20 ± 0.12	Traces	0.47 ± 0.04
		1.5	2.06 ± 0.11	16.07 ± 0.16	1.38 ± 0.21	1.60 ± 0.23	0.02 ± 0.01	0.50 ± 0.03
	60	0.5	2.13 ± 0.26	13.71 ± 0.18	1.68 ± 0.15	1.22 ± 0.14	Traces	0.46 ± 0.11
		1.0	2.68 ± 0.17	19.47 ± 0.17	1.67 ± 0.12	2.06 ± 0.21	0.22 ± 0.03	0.60 ± 0.08
		1.5	2.83 ± 0.15	20.35 ± 0.23	1.70 ± 0.13	2.59 ± 0.16	0.54 ± 0.02	0.61 ± 0.08
140	30	0.5	2.05 ± 0.15	14.44 ± 0.28	1.67 ± 0.13	0.76 ± 0.15	Traces	0.47 ± 0.06
		1.0	2.66 ± 0.08	19.98 ± 0.19	1.70 ± 0.16	2.35 ± 0.13	0.29 ± 0.02	0.63 ± 0.05
		1.5	2.93 ± 0.12	21.06 ± 0.24	1.77 ± 0.06	2.81 ± 0.04	0.70 ± 0.04	0.65 ± 0.07
	60	0.5	2.77 ± 0.06	18.57 ± 0.21	1.71 ± 0.14	2.16 ± 0.08	0.27 ± 0.07	0.60 ± 0.07
		1.0	2.87 ± 0.15	19.55 ± 0.18	1.84 ± 0.08	2.59 ± 0.15	1.14 ± 0.07	0.63 ± 0.08
		1.5	3.31 ± 0.18	19.43 ± 0.22	1.80 ± 0.15	3.01 ± 0.13	2.23 ± 0.12	0.56 ± 0.05
150	30	0.5	2.65 ± 0.09	19.40 ± 0.17	1.69 ± 0.03	1.74 ± 0.05	0.28 ± 0.06	0.63 ± 0.06
		1.0	3.21 ± 0.11	20.93 ± 0.20	1.77 ± 0.06	3.05 ± 0.14	1.26 ± 0.10	0.69 ± 0.05
		1.5	3.68 ± 0.10	19.64 ± 0.19	1.84 ± 0.05	3.11 ± 0.22	2.43 ± 0.15	0.59 ± 0.06
	60	0.5	2.75 ± 0.17	19.39 ± 0.15	1.71 ± 0.17	2.47 ± 0.18	1.08 ± 0.22	0.67 ± 0.09
		1.0	3.21 ± 0.26	16.79 ± 0.19	1.76 ± 0.22	3.21 ± 0.11	3.68 ± 0.18	0.60 ± 0.07
		1.5	4.05 ± 0.20	13.15 ± 0.21	1.48 ± 0.14	3.81 ± 0.19	5.28 ± 0.17	0.53 ± 0.07

[a] Glc, Xyl, Ara, AcA, F, HMF as glucose, xylose, arabinose, acetic acid, furfural and 5-hydroxymethylfurfural, respectively.

Table 4
Range and levels of independent process variables used in experimental design.

Variable		Range and levels				
		−α	−1	0	+1	+α
Temperature (°C)	X_1	123.2	130	140	150	156.8
Time (min)	X_2	19.8	30	45	60	70.2
Acid concentration (%)	X_3	0.2	0.5	1.0	1.5	1.8

Maximum xylose recovery (ca. 21% of dry reed stem, or 91% of total xylose) was observed when giant reed was hydrolyzed at 140 °C for 30 min in 1.5% acid solution. Under these conditions, the contents of furfural, 5-hydroxymethylfurfural, acetic acid and glucose were found as 0.7%, 0.7%, 2.8% and 2.9%, respectively, pointing to fairly good quality of xylose hydrolyzate with low concentration of inhibitors. The further hydrolysis extension up to 60 min (at fixed 140 °C) caused substantial carbohydrate degradation (2.2% of furfural, 3.0% of acetic acid and 3.3% of glucose at 1.5% acid) with respective loss in xylose recovery (yield ca. 83%).

Since the high values of xylose recovery were achieved (90% and more), the tested ranges of the principal independent process variables were later used in statistical experimental design, to maximize the reaction outputs.

3.3. Hydrolysis modeling and optimization

Statistical modeling and optimization of dilute sulfuric acid hydrolysis of giant reed stems was done using response surface methodology (RSM) (Myers, Montgomery, & Anderson-Cook, 2009). To optimize the effect of the principal independent variables (reaction time (X_1), temperature (X_2) and acid concentration (X_3)) on efficiency (Y_1) and selectivity (Y_2) of xylan conversion to xylose, the 2^3 central composite rotatable design (CCRD) was employed. The current settings of process variables (Table 4) were defined based on results of the preliminary experiments, discussed above. According to CCRD, the RSM experimental design matrix for 3 coded independent variables at 5 levels each, with 6 star (axial) points and 5 replicates at the central point (total 19 runs) was developed (Table 5) and the significant effects having the greatest impact on reaction outputs (Y_1 and Y_2) were calculated using experimental data.

In Fig. 1 the Pareto charts of standardized linear, quadratic and interaction effects of the independent process variables, sorted by their absolute magnitude in relation to the statistical significance p-level of 0.05, are shown. As can be seen, the effectiveness of xylan conversion to xylose (Fig. 1, top) is mainly affected by acid concentration (linear and quadratic effects) and in a lesser degree – by reaction temperature (quadratic effect) and interaction effect between temperature and acid concentration. The hydrolysis selectivity (Fig. 1, bottom) is primarily controlled by interaction effect between reaction temperature and acid concentration as well as by quadratic effect of acid concentration. The statistical significance of estimated effects was checked by analysis of variance (ANOVA) (Table 6). The low p-values of the main effects ($p < 0.01$) indicated high statistical significance of the estimated relations between

Table 5
Central composite rotatable design (CCRD) applied for giant reed hydrolysis and the corresponding experimental responses on xylan conversion (Y_1) and process selectivity (Y_2) used for RSM modeling.

Run N°	Coded variables			Responses	
	X_1	X_2	X_3	Y_1	Y_2
1	−1	−1	−1	0.30	3.67
2	−1	−1	+1	0.69	7.80
3	−1	+1	−1	0.59	6.42
4	−1	+1	+1	0.88	7.20
5	+1	−1	−1	0.84	7.32
6	+1	−1	+1	0.85	5.33
7	+1	+1	−1	0.84	7.04
8	+1	+1	+1	0.57	3.25
9	−α	0	0	0.65	7.14
10	+α	0	0	0.59	3.59
11	0	−α	0	0.78	7.52
12	0	+α	0	0.89	6.55
13	0	0	−α	0.15	1.90
14	0	0	+α	0.91	6.07
15 (C)	0	0	0	0.90	7.01
16 (C)	0	0	0	0.89	6.83
17 (C)	0	0	0	0.90	6.97
18 (C)	0	0	0	0.91	7.07
19 (C)	0	0	0	0.90	7.11

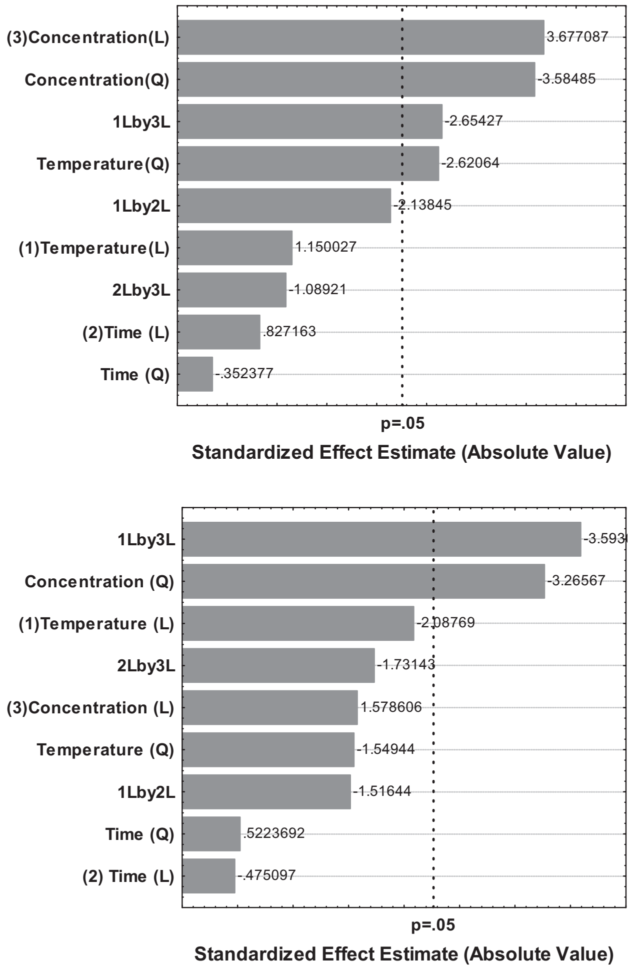

Fig. 1. Pareto charts of standardized effects for xylan conversion to xylose (top) and hydrolysis selectivity (bottom).

variables within a 99% confidence interval. To define the optimum levels (conditions) of the independent process variables, the second-order polynomial model (Eq. (1)) was fitted to experimental data and the regression coefficients were calculated by multiple regression analysis. Two model equations were obtained using more statistically significant regression coefficients ($p < 0.05$):

$$Y_1 = -25.473 + 0.3037X_1 - 0.0009X_1^2 + 0.1012X_2 + 4.7889X_3 - 0.4848X_3^2 - 0.0006X_1X_2 - 0.023X_1X_3 \qquad (2)$$

$$Y_2 = -139.117 + 1.613X_1 + 0.544X_2 + 49.652X_3 - 3.722X_3^2 - 0.267X_1X_3 \qquad (3)$$

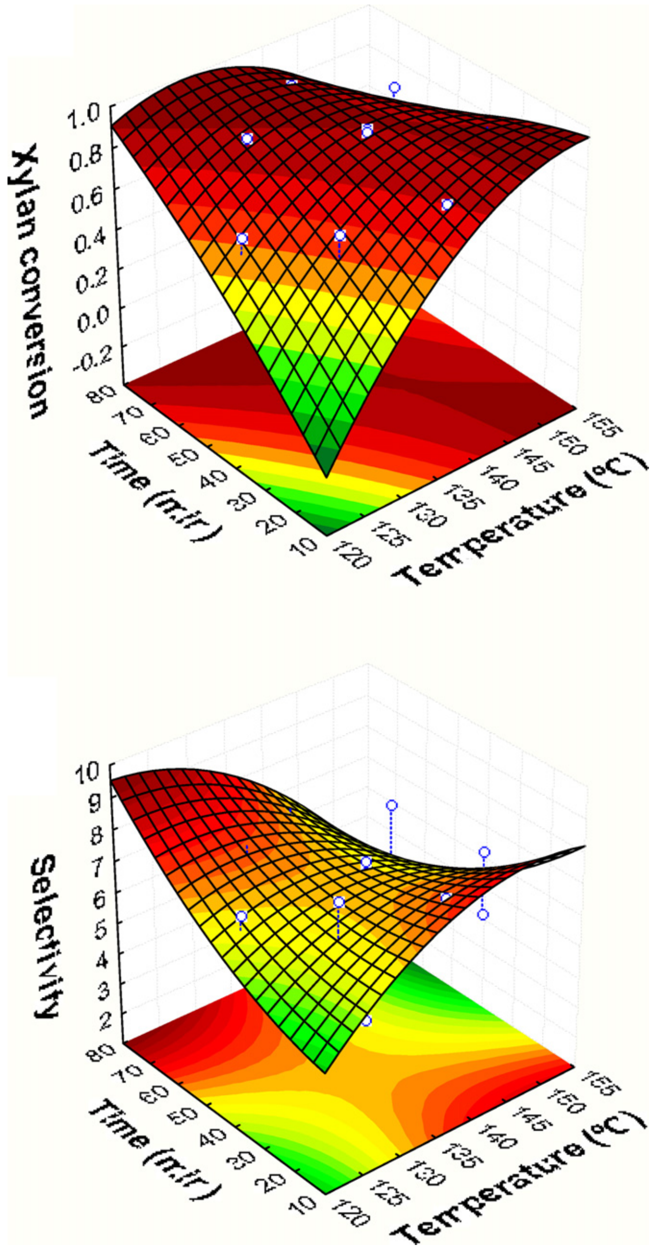

Fig. 2. Response surfaces and contour plots of modeled xylan conversion to xylose (top) and hydrolysis selectivity (bottom) as a function of reaction time (*t*, min) and reaction temperature (*T*, °C) at fixed acid concentration of 1% set as a central point.

Figs. 2–4 show the 3D response surfaces and the corresponding contour plots constructed on the basis of Eqs. (2) and (3) and illustrate the modeled effects of independent variables on reaction outputs. The response surfaces for xylan conversion (Figs. 2–4, top),

Table 6

ANOVA of estimated linear (*L*), quadratic (*Q*) and interaction effects for xylan conversion (Y_1) and process selectivity (Y_2).

Factor	Y_1				Y_2			
	Estimated effect	*t*-Test	*F*-test	*p*	Estimated effect	*t*-Test	*F*-test	*p*
(1) Temperature (*L*)	0.0777	1.1500	1.3226	0.2798	−1.1894	−2.0877	4.3584	0.0664
Temperature (*Q*)	−0.1772	−2.6206	6.8677	0.0278	−0.8829	−1.5494	2.4008	0.1557
(2) Time (*L*)	0.0559	0.8272	0.6842	0.4295	−0.2707	−0.4751	0.2257	0.6460
Time (*Q*)	−0.0238	−0.3524	0.1242	0.7327	0.2977	0.5224	0.2729	0.6140
(3) Concentration (*L*)	0.2486	3.6771	13.5210	0.0051	0.8993	1.5786	2.4920	0.1489
Concentration (*Q*)	−0.2424	−3.5849	12.8511	0.0059	−1.8609	−3.2657	10.6646	0.0098
1L by 2L	−0.1889	−2.1385	4.5730	0.0612	−1.1288	−1.5164	2.2996	0.1637
1L by 3L	−0.2344	−2.6543	7.0451	0.0263	−2.6745	−3.5931	12.9101	0.0058
2L by 3L	−0.0962	−1.0892	1.1864	0.3044	−1.2888	−1.7314	2.9979	0.1174

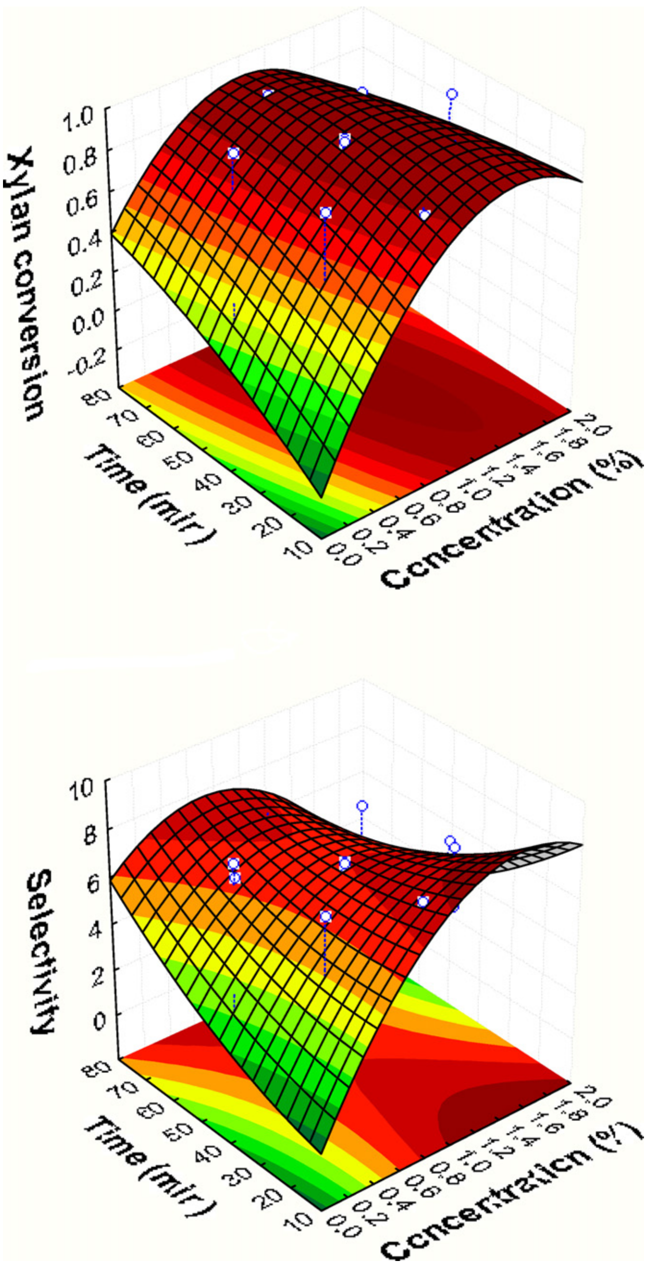

Fig. 3. Response surfaces and contour plots of modeled xylan conversion to xylose (top) and hydrolysis selectivity (bottom) as a function of reaction time (*t*, min) and acid concentration (*C*, %) at fixed reaction temperature of 140 °C set as a central point.

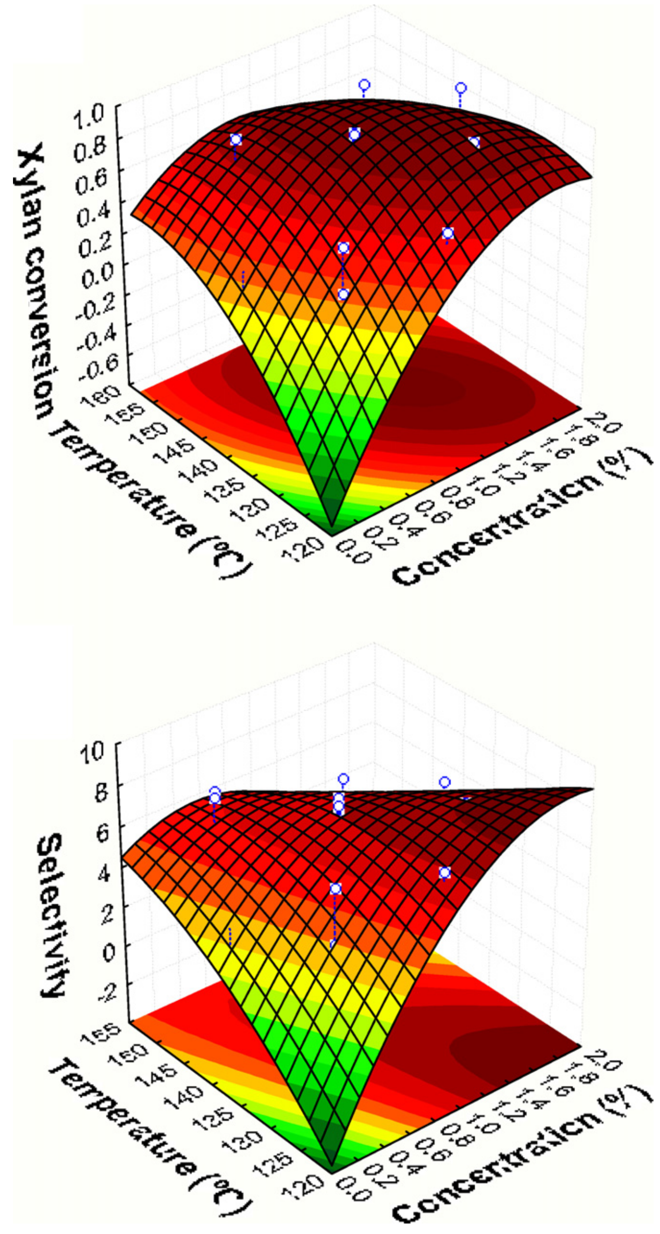

Fig. 4. Response surfaces and contour plots of modeled xylan conversion to xylose (top) and hydrolysis selectivity (bottom) as a function of reaction temperature (*T*, °C) and acid concentration (*C*, %) at fixed reaction time of 45 min set as a central point.

having some maximum values (stationary points) near the center point of the experimental design, allow locating and characterizing the optimum responses. The effect of reaction temperature and time on xylan conversion is illustrated in Fig. 2 (top). At fixed acid concentration set at 1% as a center point of statistical experimental design, the maximum xylose yield can be obtained at 140–145 °C and 35–45 min reaction time. Fig. 3 (top) shows effect of acid concentration and reaction time at constant temperature of 140 °C set as a center point. It can be seen that the concentration range of 1–1.5% and time 35–45 min are desirable to maximize the xylose recovery during hydrolysis. The desirable ranges of reaction temperature and acid concentration (140–145 °C and 1–1.5%, respectively) are particularly notable in Fig. 4 (top), where the reaction time was kept constant at 45 min. The negative interaction effect between temperature and acid concentration (reflected in Pareto chart) causes different responses in Fig. 4 (top). The positive effect of increased acid concentration can be only seen at low reaction temperatures. Under elevated temperatures, increase in medium acidity causes monosaccharide degradation and respective drop in xylose recovery.

The response surfaces for hydrolysis selectivity (Figs. 2–4, bottom) are more complex, with maximum and minimum values encountered at various combinations of independent variables. As can be seen from Fig. 2 (bottom), keeping fixed acid concentration at 1% as a center point, the maximum selectivity of ca. 9.5 can be expected during prolonged (more than 60 min) reaction under temperature below 120 °C, or, alternatively, during short (less than 15 min) hydrolysis under temperature above 140 °C. Similarly, at fixed temperature of 140 °C (Fig. 3, bottom), only long hydrolysis (60 min and more) at low acid concentration (ca. 0.6%) or short hydrolysis (less than 30 min) at high acid concentration (ca. 1.5%) can provide maximum process selectivity of ca. 9.5. However, these

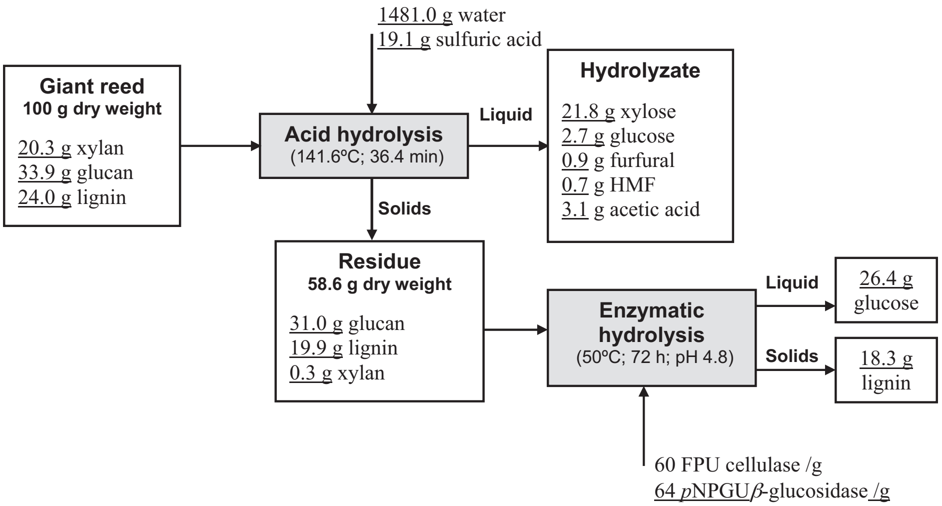

Fig. 5. Mass balance flow diagram for acid hydrolysis of giant reed (performed under optimized conditions designed for total xylan conversion to monomeric xylose) and enzymatic digestibility of unhydrolyzed solid residue.

ranges of time, temperature and acid concentration fall outside the desirable condition set specified above and needed for maximum xylan conversion to xylose. Based on Fig. 4 (bottom), the estimated selectivity level of only 7–8 (2.5–3% of glucose in solution) can be expected when hydrolysis reaction is performed under conditions designed to maximize the xylose yield in solution.

Partial differentiation of the multivariate function described by Eq. (2) was done to find an optimal combination of the independent process variables for maximum xylan conversion to xylose during hydrolysis:

$$\frac{\partial Y_1}{\partial X_1} = 0.3037 - 0.0018X_1 - 0.0006X_2 - 0.0234X_3 = 0 \tag{4}$$

$$\frac{\partial Y_1}{\partial X_2} = 0.1012 - 0.0006X_1 = 0 \tag{5}$$

$$\frac{\partial Y_1}{\partial X_3} = 4.7889 - 0.9696X_3 - 0.0234X_1 = 0 \tag{6}$$

The following optimum condition set was obtained after resolution of Eqs. (4–6): reaction time of 36.4 min, reaction temperature of 141.6 °C, sulfuric acid concentration of 1.27% and a maximum expected xylan conversion of 0.93 (or 93% of monomeric xylose recovery in solution).

To validate the developed statistical model, the replicated (4 times) control experiments were performed under established optimal conditions. The obtained experimental data on xylan conversion (0.94 ± 0.005, or 21.76 g xylose/100 g dry stem material) and hydrolysis selectivity (7.90 ± 0.106, with 2.74 g glucose/100 g dry stem material) were even superior to data predicted by model. The resulting hydrolyzate revealed low concentration of toxic substances (furfural 0.90 g, 5-hydroxymethylfurfural 0.71 g and acetic acid 3.10 g per 100 g of dry biomass) providing the high quality of xylose-rich substrate for subsequent (bio)chemical processing. The mass balance flow diagram summarizing the yields of the principal structural components (cellulose, xylan and lignin) of giant reed stem-wall material during acid hydrolysis (performed under optimized conditions) and enzymatic saccharification/digestibility of the unhydrolyzed solid residue as well (see chapter below) is shown in Fig. 5.

3.4. *Enzymatic digestibility of unhydrolyzed residue*

Solid residue after hydrolytic removal of hemicellulosic (xylan) fraction from giant reed stems essentially consists of two main components: cellulose and lignin. The subsequent fractionation/treatment of this solid residue using various chemical and biological approaches (biorefinery concept) can result in a range of high value bioproducts. Cellulose, as a more abundant and valuable chemical constituent, can be used as a source of fibers (after stems delignification), or as a source of fermentable sugars (glucose) for biofuel production (after stems enzymatic saccharification). Since hemicelluloses removal is assumed to increase the accessibility and therefore reactivity of residual lignocellulosic matrix (Sun & Cheng, 2002; Zhang, 2008), the effect of total xylan hydrolysis on enzymatic digestibility improvement of giant reed stems is of great practical interest. To assess this effect, the solid residue after dilute acid hydrolysis, performed under the optimized operation conditions, was enzymatically hydrolyzed with commercial cellulase and β-glucosidase preparations (60 FPU/g and 64 *p*NPGU/g of cellulose added, respectively) according to standard NREL procedure (Selig et al., 2008). The digestibility was expressed as a percentage of glucose released in relation to glucose loaded.

As can be seen from Table 7, the enzymatic digestibility of treated (pre-hydrolyzed) biomass was significantly improved over the control (untreated) samples. About 70% of cellulose was converted to monomeric glucose (26.4 g Glc per 100 g of dry biomass, Fig. 5) after 72 h enzymatic hydrolysis of pre-hydrolyzed reed stems, while cellulose conversion of untreated stems was only ca. 9% at the same conditions, i.e., almost 8 times less. Obviously, the recalcitrant structure of the cell-wall material in lignocellulosics, caused by strong interaction between lignin and carbohydrates (basically hemicelluloses) (Fengel & Wegener, 1989), does not permit effective enzymatic attack and saccharification of cellulose, due to limited access of enzymes to active reaction centers on the surfaces of cellulosic microfibrils. Acidic removal of hemicellulosic polysaccharides destroys the lignin-carbohydrate matrix shielding cellulose microfibrils in the cell walls, thereby substantially increasing digestibility of cellulose in enzymatic hydrolysis.

Table 7
Enzymatic digestibility improvement of giant reed stem-wall material after dilute sulfuric acid hydrolysis under found optimum conditions.

	Enzymatic digestibility (%)		
	24 h	48 h	72 h
Untreated	8.13 ± 0.13	8.93 ± 0.02	9.35 ± 0.13
Treated	65.15 ± 0.19	68.27 ± 0.49	70.23 ± 0.80

The degree of cellulose conversion to fermentable sugars can be further improved by optimization study of enzymatic saccharification of the pre-hydrolyzed giant reed stems in terms of enzyme load and process duration. This study is currently under performance in our research group.

4. Conclusions

The low temperature dilute sulfuric acid hydrolysis was very effective to convert the giant reed (*A. donax* L.) heteroxylan to monomeric sugars providing a quality xylose-rich substrate for subsequent (bio)chemical processing and reactive hemicellulose-free solid residue ready for further fractionation within complex biorefinery scheme. The statistical modeling using response surface methodology made it possible to identify the main factors of the multi-variable hydrolysis process affecting efficiency and selectivity of xylan conversion to xylose and to define the optimum set of reaction conditions for maximal xylose recovery in solution. Under optimum reaction conditions (141.6 °C; 36.4 min and 1.27% acid concentration) the high xylan conversion of 0.94 (94% of xylose recovery or 21.76 g/100 g giant reed) was achieved vs. 0.93 predicted by model, with limited cellulose degradation and furans formation. The solid cellulosic residue after hydrolysis can be easy converted to fermentable sugars (glucose) by enzymatic saccharification, providing degree of cellulose digestibility of 70% vs. 9% for untreated biomass.

Acknowledgements

The financial support of the Fundação para a Ciência e a Tecnologia (FCT, Portugal) within research contract PTDC/AGR-CFL/103840/2008 is gratefully acknowledged. The authors thank D. Neiva and Dr. L. Duarte for their technical assistance.

References

Akpinar, O., Levent, O., Bostanci, S., Bakir, U., & Yilmaz, L. (2011). The optimization of dilute acid hydrolysis of cotton stalk in xylose production. *Applied Biochemistry Biotechnology*, *163*, 313–325.

Atchison, J. E. (1987). Data on non-wood plant fibers. In F. Hamilton, B. Leopold, & M. J. Kocurek (Eds.), *Pulp and paper manufacture. Secondary fibers and non-wood pulping* (pp. 4–16). Atlanta, Montreal: TAPPI, CPPA.

Bassoa, M. C., Cerrellaa, E. G., Buonomoa, E. L., Bonellia, P. R., & Cukiermana, A. L. (2005). Thermochemical conversion of *Arundo donax* into useful solid products. *Energy Sources*, *27*, 1429–1438.

Berghem, L. E. R., & Petterson, L. G. (1974). The mechanism of enzymatic cellulose degradation. Isolation and some properties of a β-glucosidase from *Trichoderma viride*. *European Journal Biochemistry*, *46*, 295–305.

Browning, B. L. (1967). *Methods of wood chemistry* John Wiley & Sons: New York.

Caparrós, S., Ariza, J., Hernanz, D., & Díaz, M. J. (2006). *Arundo donax* L. valorization under hydrothermal and pulp processing. *Industrial Engineering Chemistry Research*, *45*, 2940–2948.

Caparrós, S., Garrote, G., Ariza, J., & López, F. (2006). Autohydrolysis of *Arundo donax* L., a kinetic assessment. *Industrial Engineering Chemistry Research*, *45*, 8909–8920.

Dien, B. S., Jung, H.-J. G., Vogel, K. P., Casler, M. D., Lamb, J. F. S., Iten, L., et al. (2006). Chemical composition and response to dilute-acid pretreatment and enzymatic saccharification of alfalfa, reed canarygrass, and switchgrass. *Biomass and Bioenergy*, *30*, 880–891.

Esteghlalian, A., Hashimoto, A. G., Fenske, J. J., & Penner, M. H. (1997). Modeling and optimization of the dilute-sulfuric-acid pretreatment of corn stover, poplar and switchgrass. *Bioresource Technology*, *59*, 129–136.

Fengel, D., & Wegener, G. (1989). *Wood: Chemistry, ultrastructure, reactions*. New York, Berlin: Walter de Gruyter.

Fernando, S., Adhikari, S., Chandrapal, C., & Murali, N. (2006). Biorefineries: Current status, challenges, and future direction. *Energy Fuels*, *20*, 1727–1737.

FitzPatrick, M., Champagne, P., Cunningham, M. F., & Whitney, R. A. (2010). A biorefinery processing perspective: Treatment of lignocellulosic materials for the production of value-added products. *Bioresource Technology*, *101*, 8915–8922.

Ghose, T. K. (1987). Measurement of cellulase activities. *Pure Applied Chemistry*, *59*, 257–268.

Granström, T. B., & Leisola, M. (2009). Production and applications of xylitol. *Agro Food Industry Hi-Tech*, *20*, 27–31.

Guo, G.-L., Chen, W.-H., Chen, W.-H., Men, L.-C., & Hwang, W.-S. (2008). Characterization of dilute acid pretreatment of silvergrass for ethanol production. *Bioresource Technology*, *99*, 6046–6053.

Hidalgo, M., & Fernandez, J. (2001). Biomass production of ten populations of giant reed (*Arundo donax* L.) under the environmental conditions of Madrid (Spain). In S. Kyritsis, A. A. C. M. Beenackers, P. Helm, A. Grassi, & D. Chiaramonti (Eds.), *Biomass for energy and industry, proceedings of 1st world conference, Sevilla, Spain, 5–9 June 2000* (pp. 1881–1884). London: James & James Science Publishers Ltd.

Hurter, A. M. (1988). Utilization of annual plants and agricultural residues for the production of pulp and paper. In *Proceedings TAPPI pulping conference, book 1* New Orleans, LA, USA, (pp. 139–160).

Jeong, T.-S., Um, B.-H., Kim, J.-S., & Oh, K.-K. (2010). Optimizing dilute-acid pretreatment of rapeseed straw for extraction of hemicellulose. *Applied Biochemistry Biotechnology*, *161*, 22–33.

Joseleau, J. P., & Barnoud, F. (1975). Hemicelluloses of *Arundo donax* at different stages of maturity. *Phytochemistry*, *14*, 71–75.

Kamm, B., Schneider, B. U., Hüttl, R. F., Grünewald, H., Gusovius, H.-J., Stollberg, C., et al. (2006). Lignocellulosic feedstock biorefinery – Combination of technologies of agroforestry and a biobased substance and energy economy. *Forum der Forschung*, *19*, 53–62.

Kamm, B., & Kamm, M. (2007). Biorefineries – Multi product processes. *Advances Biochemical Engineering Biotechnology*, *105*, 175–204.

Lewandowski, I., Scurlock, J. M. O., Lindvall, E., & Christou, M. (2003). The development and current status of perennial rhizomatous grasses as energy crops in the US and Europe. *Biomass and Bioenergy*, *25*, 335–361.

Lewis, M., & Jackson, M. (2002). Nalgrass: A nonwood fiber source suitable for existing US pulp mills. In J. Janick, & A. Whipkey (Eds.), *Trends in new crops and new uses* (pp. 371–376). Alexandria, VA: ASHS Press.

Martinez, A., Rodriguez, M. E., York, S. W., Preston, J. F., & Ingram, L. O. (2000). Use of UV absorbance to monitor furans in dilute acid hydrolysates of biomass. *Biotechnology Progress*, *16*, 637–641.

Miller, G. L. (1959). Use of dinitrosalicylic reagent for determination of reducing sugars. *Analytic Chemistry*, *31*, 426–428.

Myers, R. H., Montgomery, D. C., & Anderson-Cook, C. M. (2009). *Response surface methodology: Process and product optimization using designed experiment* (3rd ed.). New York: John Wiley & Sons.

Perdue, R. E. (1958). *Arundo donax* – source of musical reeds and industrial cellulose. *Economic Botany*, *12*, 368–404.

Rahman, S. H. A., Choudhury, J. P., Ahmad, A. L., & Kamaruddin, A. H. (2007). Optimization studies on acid hydrolysis of oil palm empty fruit bunch fiber for xylose production. *Bioresource Technology*, *98*, 554–559.

Saha, B. C. (2003). Hemicellulose bioconversion. *Journal Industrial Microbiology Biotechnology*, *30*, 279–291.

Selig, M., Weiss, N., & Ji, Y. (2008). Enzymatic saccharification of lignocellulosic biomass. *Laboratory analytical procedure, NREL/TP-510-42629 Standard*.

Shatalov, A. A., Quilhó, T., & Pereira, H. (2001). *Arundo donax* L. reed: New perspectives for pulping and bleaching – 1. Raw material characterization. *TAPPI Journal*, *84*, 1–12.

Shatalov, A. A., & Pereira, H. (2006). Papermaking fibers from giant reed (*Arundo donax* L.) by advanced ecologically friendly pulping and bleaching technologies. *BioResources*, *1*, 45–61.

Shatalov, A. A., & Pereira, H. (2007). Polysaccharide degradation during ozone-based TCF bleaching of non-wood organosolv pulps. *Carbohydrate Polymers*, *67*, 275–281.

Sun, Y., & Cheng, J. (2002). Hydrolysis of lignocellulosic materials for ethanol production: A review. *Bioresource Technology*, *83*, 1–11.

Verteris, C., Georghiou, K., Christodoulakis, N., Santas, P., & Santas, R. (2004). Fiber dimensions, lignin and cellulose content of various plant materials and their suitability for paper production. *Industrial Crops Products*, *19*, 245.

Zhang, Y.-H. P. (2008). Reviving the carbohydrate economy via multi-product lignocellulose biorefneries. *Journal Industrial Microbiology Biotechnology*, *35*, 367–375.